

Original Research

# Bioinformatics and Experimental Identification of *circ\_0001535* Associated with Diagnosis and Development of Alzheimer's Disease

Mingming Ma<sup>1</sup>, Dandan Xie<sup>2</sup>, Jing Zhao<sup>1,\*</sup><sup>1</sup>Department of Neurology, Hangzhou Red Cross Hospital, 310000 Hangzhou, Zhejiang, China<sup>2</sup>Department of Sports Rehabilitation, Hangzhou Red Cross Hospital, 310000 Hangzhou, Zhejiang, China\*Correspondence: [3453986521@qq.com](mailto:3453986521@qq.com) (Jing Zhao)

Academic Editor: Gernot Riedel

Submitted: 10 October 2022 Revised: 21 December 2022 Accepted: 28 December 2022 Published: 26 July 2023

## Abstract

**Background:** Alzheimer's disease (AD) is a type of disease frequently occurs in the elderly population. Diagnosis and treatment methods for this disease are still lacking, and more research is required. In addition, little is known about the function of the circular RNAs (circRNAs) in AD. **Methods:** In this research, RNA expression data of AD from the Gene Expression Omnibus (GEO) database were downloaded. The expression levels of circRNAs in cerebrospinal fluid samples of healthy participants and AD patients were measured by reverse transcription-quantitative PCR (RT-qPCR). The diagnosed value of differential expressed circRNAs was analyzed with the Receiver operating characteristic curve (ROC). Pathways related to *circ\_0001535* were found using gene set enrichment analysis (GSEA) and Metascape. The direct interactions between *circ\_0001535* and E2F transcription factor 1 (*E2F1*) or E2F1 and dihydrofolate reductase (*DHFR*) were verified using Chromatin immunoprecipitation (ChIP) and RNA Binding Protein Immunoprecipitation (RIP) assays. Cell Counting Kit-8 (CCK8) and flow cytometry were used to identify the function of *circ\_0001535/E2F1/DHFR* axis on the proliferation and apoptosis of AD cells. **Results:** In total, 12 circRNAs have been linked to AD diagnosis. The expression levels of 7 circRNAs differed between AD patients and control groups. *Circ\_0001535* had the most diagnose value among these circRNAs. Hence, *circ\_0001535* was regarded as a key circRNA in the present study. *E2F1/DHFR* axis was predicted to be regulated by *circ\_0001535*. In addition, IP assays experiment results showed that E2F1 could bind to the promoter region of *DHFR* and be regulated by *circ\_0001535*. *In vitro* results showed that *circ\_0001535* overexpression could promote *DHFR* expression, while *E2F1* knock down could inhibit *DHFR* expression in SH-SY5Y cells. Finally, rescue experiments suggested that *circ\_0001535* could reduce A $\beta$ 25-35-induced SH-SY5Y cell proliferation and facilitate apoptosis through *E2F1/DHFR* axis. **Conclusions:** Our research in AD circRNA can offer important information regarding the role of specific circRNAs in the AD environment and point to specific future areas of therapeutic intervention in AD.

**Keywords:** Alzheimer's disease; bioinformatic analyze; *circ\_0001535*; E2F transcription factor 1; dihydrofolate reductase; apoptosis

## 1. Introduction

Alzheimer's disease (AD) is the most common cause of dementia, rapidly becoming one of the most costly and burdensome diseases in the twenty-first century [1]. The incidence of this disease is increasing every year. Some reports estimate that by 2050, there will be more than 80 million AD patients worldwide [2,3]. Studies have suggested that AD is a complex neurodegenerative disease with multiple pathophysiologies. AD development is associated with  $\beta$ -amyloid and neurofibrillary tangles (NFTs). Many clinical trials have focused on reducing  $\beta$ -amyloid [4]. Although studies on AD have been widely reported, its current treatment for AD is still only to improve symptoms and eliminate A $\beta$ , with no effective treatment [5]. Therefore, it is critical to search for new therapeutic targets in the pathogenesis of Alzheimer's disease.

Current researchers believed that AD is probably caused by the interaction between three different factors: genetic, environmental, and epigenetic [6,7]. Recent studies have found that non-coding RNAs play an important role in epigenetic regulation [8]. For example, some re-

searchers found that microRNA (*miR*)-143-3p could regulate the expression of Death-associated Protein Kinase 1 (*DAPK1*) to inhibit Tau phosphorylation in AD [9]. *MiR-22-3p* in AD also regulates Sex Determining Region Y Box Protein 9 (*SOX9*) [9]. In addition, Metastasis Associated Lung Adenocarcinoma Transcript 1 (*MALAT1*) is a long non-coding RNA (lncRNA) that has been shown to regulate the expression of Erythropoietin-producing Hepatocellular Receptor A2 (*EPHA2*) in AD via *miR-200a* [10]. These reports indicate that non-coding RNAs play essential roles in regulating AD pathogenesis and detecting prognosis. On the other hand, more non-coding RNAs, including circular RNAs (circRNAs), need to be discovered and proven.

CircRNAs are new non-coding RNAs discovered recently, and their structures are highly evolutionarily conserved [11]. In brain tissue, the expression of circRNAs also changes with neuronal differentiation. Alterations in circRNAs expression levels have been described in different neurological diseases, such as Parkinson's disease (PD) and AD [12–15]. In PD, circRNAs were suggested to play crucial regulatory roles in regulating dopaminergic neuron



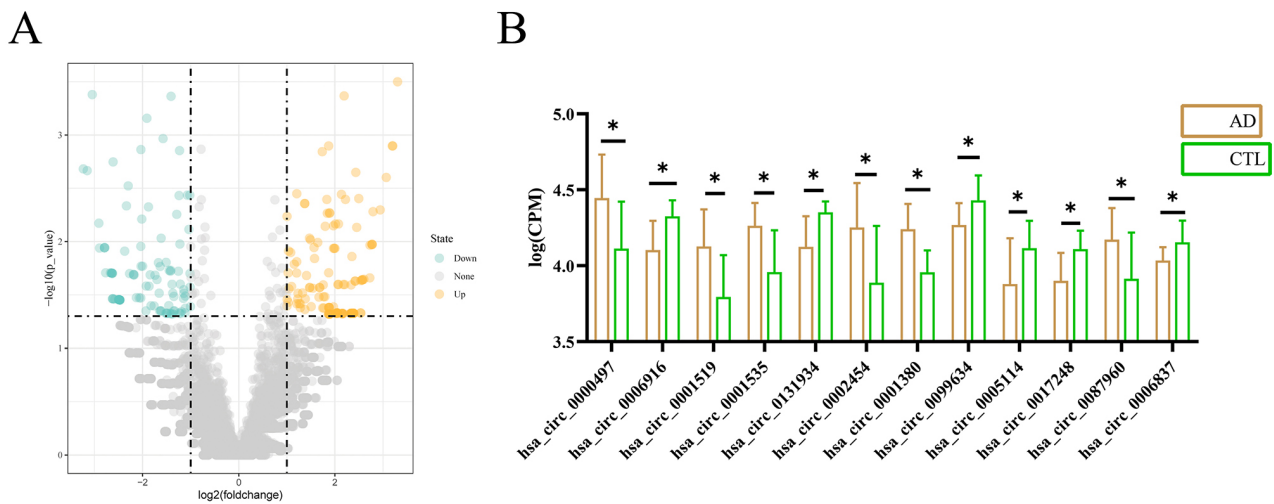


**Fig. 1. Differential expression analysis of circRNA between Alzheimer's disease (AD) and Health donors.** (A) Volcano plot shows differential expressed circRNAs. (B) Differential expression analysis of 12 circRNAs between AD and Health groups. \* $p < 0.05$  compared with control (CTL) group. CPM, count-per-million.

injury, neuron degeneration, and neurotoxic effect [16,17]. Similarly, some circRNAs may contribute to transcription regulation in AD and provide potential biomarkers for AD diagnosis and treatment [18]. Ren and his partners [19] constructed a six-circRNA panel which was an AD-specific and a promising biomarker of AD. Some circRNAs in the parahippocampal gyrus have also been regarded as possible biomarkers and regulators of AD [20]. *Circ\_0049472* may be involved in AD pathogenesis and mediated A $\beta$ -induced neurotoxicity [21]. *Circ\_HUWE1* has also been proved that it knockdown alleviated Amyloid- $\beta$ -Induced Neuronal Injury in SK-N-SH Cells [22]. Although circRNA is intimately linked to Alzheimer's disease, more research is needed to determine the underlying mechanisms for the involvement of new circRNAs in AD.

This study aimed to identify key circRNAs related to AD pathogenesis. The expression levels of 7 circRNAs were significantly different between the control group and AD patients. They also had high diagnostic ability in AD. Among these circRNAs, *circ\_0001535* had the largest Area Under Curve (AUC) value and the expression level of *circ\_0001535* was most significantly different between the control group and the AD patient group. Previous studies have reported that *circ\_0001535* was differentially expressed in some malignancies [23–25]. *Circ\_0001535* could regulate colorectal cancer progression via *miR-433-3p/Recombination signal-binding protein J $\kappa$  (RBPJ)* axis [23]. There was an increasing trend in *circ\_0001535* level for Hepatocellular Carcinoma from normal samples to tumor tissues [25]. However, there are few studies on *circ\_0001535* in AD. Hence, we regarded *circ\_0001535* as a key circRNA in the current study. Pathway enrichment analysis and JASPAR analysis were performed to reveal the gene targets. Moreover, our analysis and experiments revealed that *circ\_0001535* might affect dihydrofolate reduc-

tase (*DHFR*) transcription by regulating E2F transcription factor 1 (*E2F1*) during the development of AD.

## 2. Materials and Methods

### 2.1 Data Collection and Patient Selection

For bioinformatics analysis, raw sequencing data of RNA-seq and relative metadata were obtained from Gene Expression Omnibu (GEO) database (GSE104704, <https://www.ncbi.nlm.nih.gov/geo/query/acc.cgi?acc=GSE104704>), and RNA expression levels of genes in the lateral temporal lobe of the patients were sequenced by Illumina NextSeq 500 platform. In addition, the diagnosis information of participants from two groups, elderly control (Control) and AD, were obtained for further research. For clinical experiments, patients were diagnosed with AD in our hospital were enrolled [26]. Controls refer to participants who were examined due to transient neurologic symptoms. Cerebrospinal fluid was drawn through lumbar puncture from the space between L3-L4 or L4-L5 and stored at  $-80^{\circ}\text{C}$ . The study protocol was approved by the Medical Ethics Committee of Red Cross Hospital (Approval NO: 202280).

### 2.2 Data Preprocessing

RNA-sequencing data were downloaded from the GEO database and converted to FASTQ files by using SRAtoolkit software (version 3.0.1, National Institutes of Health, Bethesda, MD, USA). Gene expression data were directly downloaded from supplemental data in GSE104704. CircRNA expression levels were predicted with CIRCexplorer software (version 2.0, CIRCexplorer, Shanghai, China). Briefly, FASTQ files were mapped to human genome HG19 with STAR aligner. The alignment process produced BAM files and Chimeric junction files.

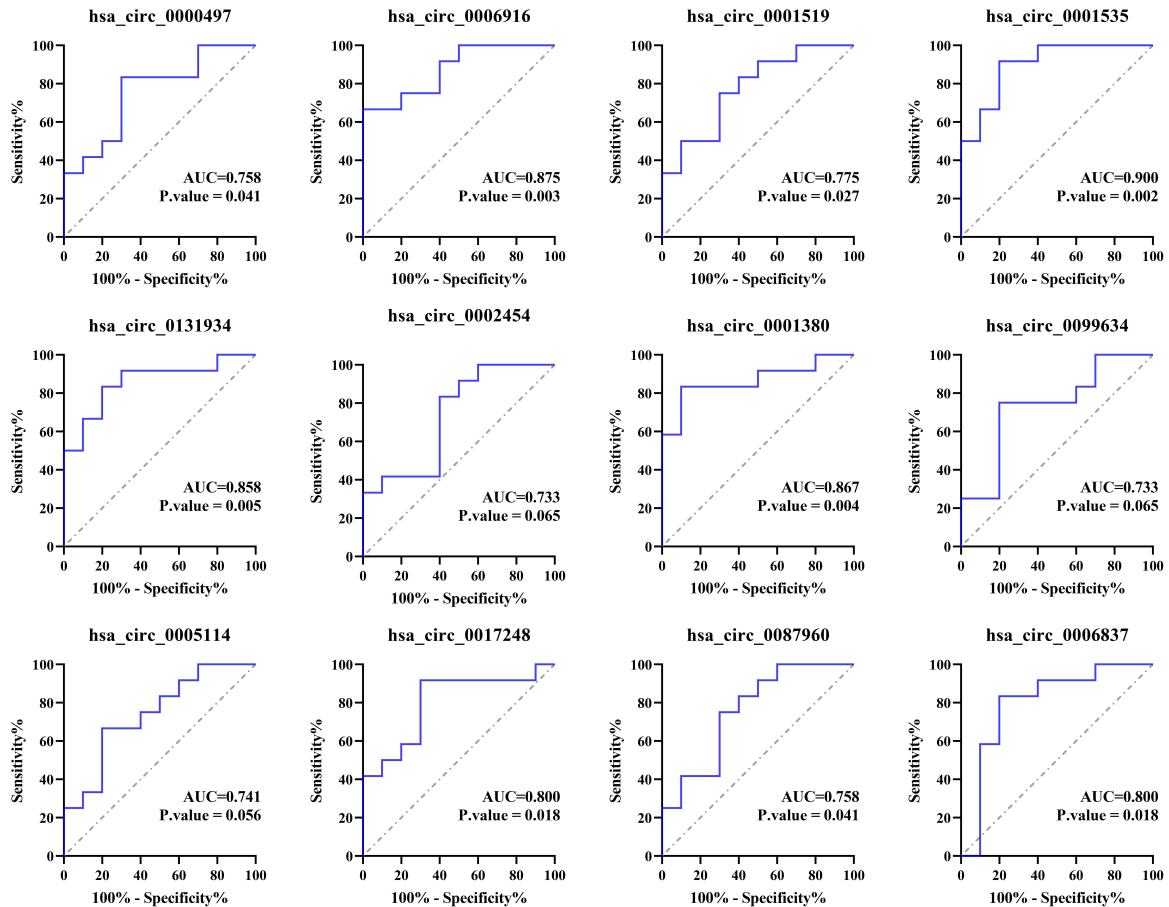


**Fig. 2. ROC curve of 12 representative circRNAs.** ROC, receiver operating characteristic curve; AUC, area under curve.

Chimeric junction files were parsed by using the CIRCexplorer2 parse module. Then, the Browser Extensible Data (BED) file containing the subsequent connection information is created. BED files were annotated with reference genome HG19, and results containing circRNA expression and annotation files were saved.

### 2.3 Differential Expression Analysis

Differential expression analysis and normalization of circRNA expression data were processed using R package *edgeR*. Results were visualized with a volcano plot. CircRNAs with low expression were removed. Expression levels of filtered circRNAs were then visualized using a boxplot.

### 2.4 Receiver Operating Characteristic Curve (ROC) Analysis

The ROC curve was used to evaluate the diagnostic value of differentially expressed circRNAs. Briefly, 12 ROC curves were plotted using GraphPad Prism (version 8.0, GraphPad Software, San Diego, CA, USA), circRNA with the highest AUC was thought to have crucial diagnostic value for AD.

### 2.5 Pathway Enrichment Analysis

Gene Set Enrichment Analysis (GSEA) and Metascape pathway enrichment analysis were processed separately. The pathways affected by circRNA signature were searched using GSEA (version 4.3.2, Broad Institute, Cambridge, MA, USA). Patients with low and high *circ\_0001535* expression were divided into two groups by median. Then, GSEA was processed to screen for pathway activity difference. Pathways with  $p$  value  $< 0.05$  were considered significantly enriched. After screening for key pathways affected by *circ\_0001535*, Metascape was used to analyze the relationship between mRNA and circRNA. Briefly, Pearson's correlation score between each mRNA and *circ\_0001535* was calculated. Gene which significantly correlated to *circ\_0001535* expression was obtained and listed on the Metascape website (<https://metascape.org/gp/index.html#/main/step1>). The results were downloaded from the webpage of the Metascape website.

### 2.6 JASPAR Analysis

The binding motif sequence between transcription factors and targeted genes was predicted using the JASPAR webpage (<http://jaspar.genereg.net/>). The gene symbol of the transcription factor was first searched in the JASPAR

webpage and selected for use. The transcription start site (TSS) region of targeted mRNA was downloaded from National Center for Biotechnology Information (NCBI) database and uploaded to the JASPAR database. Binding sites between transcription factor and mRNA transcription start site (TSS) region were predicted automatically.

### 2.7 Cell Culture and Transfection

Human neuroblastoma cells SH-SY5Y were purchased (BeNa Culture Collection, Beijing, China). SH-SY5Y cell line was authenticated at Meisen Biotech Co., Ltd. by short tandem repeat (STR) profiling. No contamination of mycoplasma has been identified by the company. SH-SY5Y cells were cultured in the Dulbecco's modified Eagle's medium (DMEM) (Invitrogen, Carlsbad, CA, USA) including 10% heat-inactivated fetal calf serum (FBS) and 1% Penicillin/streptomycin (P/S). Cells were cultured at 37 °C in humidified 5% CO<sub>2</sub>. In order to construct an AD cell model, cells were treated with 20 μmol/L Aβ<sub>25-35</sub> (HY-P0128, MedChemExpress, Monmouth Junction, NJ, USA). Overexpression (oe)-NC and oe-*circ\_0001535* were all purchased from RiboBio in Guangzhou. Small interfering (si)-*E2F1*, si-*DHFR* and si-NC were all purchased from RiboBio in Guangzhou. Cell transfection was done using Lipofectamine® 2000 (11668019, Thermo Fisher Scientific, Waltham, MA, USA).

### 2.8 Chromatin Immunoprecipitation (ChIP) and RNA Binding Protein Immunoprecipitation (RIP) Assay

ChIP assays were performed using a ChIP kit (ab500, Abcam, Burlingame, CA, USA), following according to the manufacturer's instructions. Briefly, SH-SY5Y cells were harvested and sonicated to chromatin. The anti-E2F1 antibody (ab245308, Abcam, Burlingame, CA, USA) was added to form the antibody-target protein-DNA complex, and protein A-Sepharose beads were used to immunoprecipitate the complex. Reverse transcription-quantitative PCR (RT-qPCR) was performed to detect the binding site. Primers used in ChIP-qPCR were as follows, Site 1 Primer: forward: 5'-GGTGAGTTGTGGGGGATTCT-3' and reverse: 5'-CCATCACCTATAGGGGGCCA-3'; Site 2 Primer: forward: 5'-TACGTCAGGCCTTCTCAGAGT-3' and reverse: 5'-ATCCCCACAACCTACCAGA-3'. Magna RIP kit (Millipore, Billerica, MA, USA) was used to process the RIP assay. Briefly, the magnetic beads were incubated with anti-E2F1 antibodies (ab245308, Abcam, Burlingame, CA, USA) or IgG-negative control antibodies (ab172730, Millipore, Billerica, MA, USA). RT-qPCR was used to detect the expression of *circ\_0001535* and *DHFR*.

### 2.9 RNA Extraction and qPCR Assay

Total RNA was extracted from Cerebrospinal fluid samples or cells with QIAamp RNeasy Micro Kit (74034, Qiagen, Dusseldorf, German). Reverse transcription was

**Table 1. The chromosomal locations and differential expression levels of circRNAs.**

Position	circbase ID	logFC	p-value
chr13:78293666-78327493+	circ_0000497	-0.78525	0.00136
chr5:78734832-78752841-	circ_0006916	0.750728	0.004062
chr5:109049220-109065214+	circ_0001519	-0.82417	0.004711
chr5:137320945-137324004-	circ_0001535	-0.70188	0.007307
chr6:54013853-54095715+	circ_0131934	0.700392	0.009089
chr1:65830317-65831879+	circ_0002454	-0.69677	0.009197
chr3:196118683-196129890-	circ_0001380	-0.712	0.01205
chr12:97886238-97954825+	circ_0099634	0.594062	0.015363
chr8:105080739-105161076+	circ_0005114	0.67712	0.017131
chr1:243736227-244006584-	circ_0017248	0.634202	0.029285
chr9:113734352-113735838-	circ_0087960	-0.58168	0.03203
chr1:8555122-8617582-	circ_0006837	0.55781	0.040893

chr, chromosomal; FC, fold change; circ, circular.

performed using 1 μg total RNA as the template and Advantage RT-for-PCR Kit (639505, Takara, shiga, Japan). Relative expression levels of genes were detected by RT2 SYBR® Green qPCR Mastermixes (330509, Qiagen, Dusseldorf, German). Primer sets for qPCR are listed in **Supplementary Table 1**. The relative expression of cDNA was normalized to GAPDH and quantified using the 2<sup>-ΔΔCt</sup> cycle threshold method.

### 2.10 Cell Counting Kit-8 (CCK-8) Assay

CCK-8 assay was used to detect cell proliferation. AD cells were seeded in 96 well plates and assayed at 0-, 24-, 48- and 72-hours using CCK-8 Kit (ab228554, Abcam, Burlingame, CA, USA), following the manufacturer's instructions. Cell viability was detected by using a microplate reader at 450 nm.

### 2.11 Apoptosis Assay

Flow cytometry was performed by using Alexa Fluor 488 Annexin V/Dead Cell Apoptosis Kit (V13241, Thermo Fisher Scientific, Waltham, MA, USA) following manufacturer's instructions. For cell apoptosis analysis, cells were harvested and fixed in pre-cold 70% ethanol at 4 °C overnight. The cells were stained with Annexin V-FITC and propidium iodide (PI) and subsequently the ratio of apoptotic cells was tested by flow cytometry (BD FACS Calibur, Becton Dickinson, Franklin Lake, NJ, USA).

### 2.12 Statistical Analysis

Differences between two or multiple groups were conducted using the Student's *t*-test or one-way analysis of variance (ANOVA) followed by a post hoc Tukey's test. Bioinformatics analysis was undertaken using R software (version 3.6.3, Statistics Department of the University of Auckland, Auckland, CA, USA) and GraphPad Prism (version 8.0, GraphPad Software, San Diego, CA, USA). *p* < 0.05 were considered statically significant.

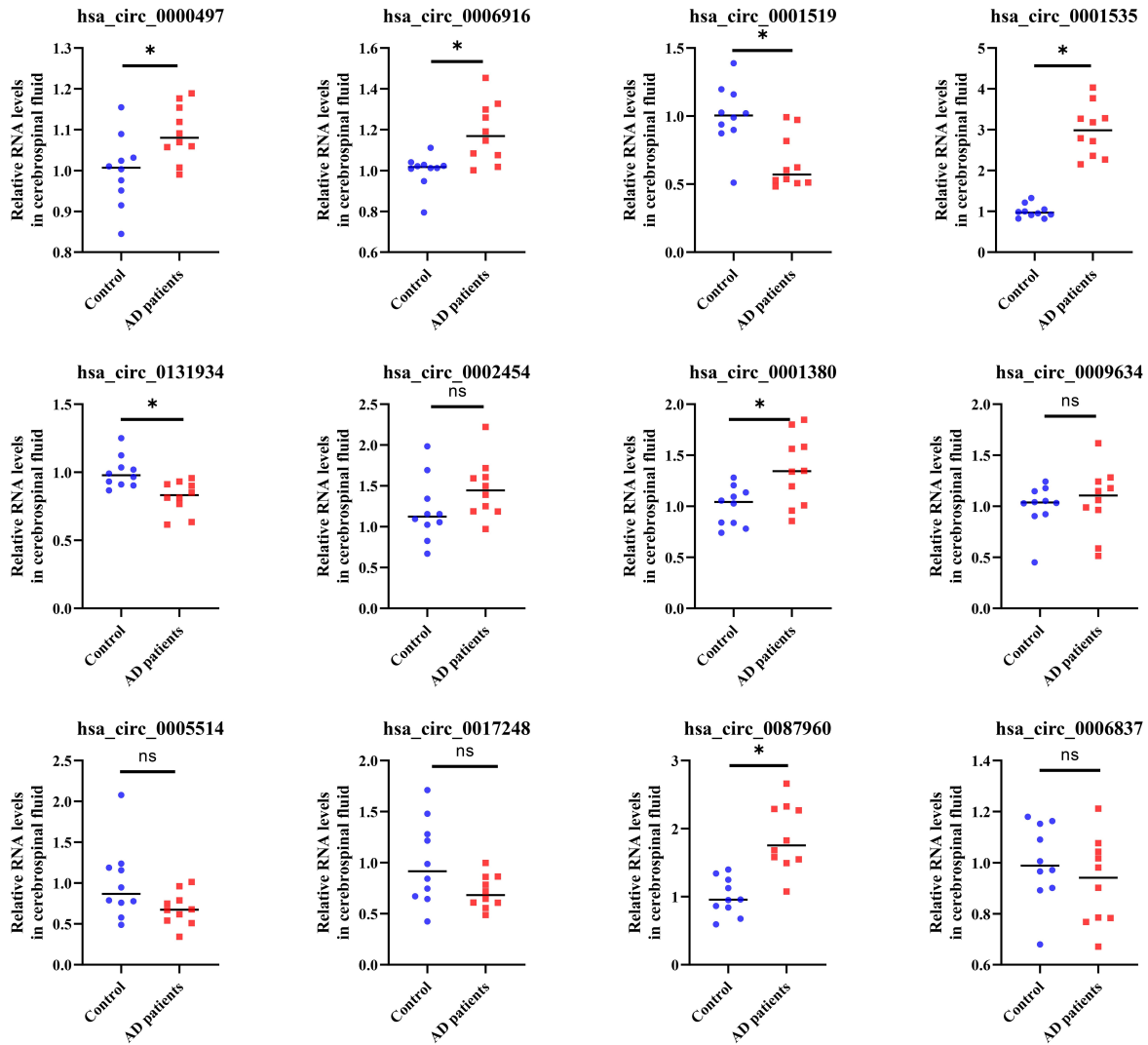


**Fig. 3.** The expression levels of 12 circRNAs in cerebrospinal fluid of AD and control group were detected by RT-qPCR. ns, no significant difference compared with Control group; \* $p < 0.05$  compared with Control group. RT-qPCR, reverse transcription-quantitative PCR.

### 3. Results

#### 3.1 Analysis of AD-Associated RNA-Seq Datasets to Identify circRNAs

To select circRNA associated with AD pathology, we searched the literature for studies reporting RNA-seq analysis of AD patients and matched controls, and we focused on studies of human brain tissue of the lateral temporal lobe. GSE104704 was selected for brain tissue RNA-seq analysis. In total, 22 brain samples were examined, including 10 cognitively normal-aged brains, and 12 AD brains. 42,504 circRNA were selected (Supplementary Table 2). Among them, 4553 known circRNAs (Supplementary Table 3) were identified using CiRCexvoer2 software (version 2.0, CiRCexplorer, Shanghai, China).

#### 3.2 Analysis of circRNAs Differentially Abundant in AD Old Brain Compared with Control Old Brain

Using edgeR to analyze the difference in expression of the above-screened circRNAs, we set at least 2-fold change thresholds in both expression aspects to draw volcano maps. In total, 135 circRNAs were found to be higher than the control and 102 lower than the control (Fig. 1A). CircRNAs with too low expression in AD patient group or control group were subsequently removed using the automatic filtering function of edgeR, which finally left 12 circRNAs with a significantly different expression between control and AD patient group. As shown in the Table 1, the chromosomal location of the parental gene where the circRNA was located. CircbaseID and  $p$  value were recorded. Compared to the expression levels in control group, the expression levels of *circ\_0000497*, *circ\_0001519*, *circ\_0001535*, *circ\_0002454*, *circ\_0001380* and *circ\_0087960* were up-regulated in AD group ( $p$

< 0.05). The expression levels of *circ\_0006916*, *circ\_0131934*, *circ\_0099634*, *circ\_0005114*, *circ\_0017248* and *circ\_0006837* were down-regulated (Fig. 1B,  $p < 0.05$ ).

### 3.3 Compare the Predictive Ability of 12 circRNAs for AD in Patients

To assess the predictive ability of 12 circRNAs for AD, we used the ROC curve of gene expression abundance to calculate the AUC and significance (Fig. 2). The AUC of all 12 circRNAs was greater than 0.7. Except for *circ\_0005114*, the  $p$  value of the other 11 circRNAs was less than 0.05. Among these circRNAs, *circ\_0001535* had the largest AUC value of 0.900 and a  $p$  value of 0.002 (Fig. 2). Overall, all 12 circRNAs performed well in determining AD, with *circ\_0001535* performing best in determining whether the sample had AD. In addition, the detection of circRNA expression levels in clinically collected samples from AD patients and healthy samples revealed that the level of *circ\_0001535* in the AD group was about three times higher than that in the healthy group, most significant in 12 circRNAs (Fig. 3,  $p < 0.01$ ).

### 3.4 Searching for Potential Pathways that were Related to *circ\_0001535*

In order to investigate the possible pathways affecting the differential expression of *circ\_0001535* in AD patients, AD patients were first divided into high and low-expression groups according to the median expression of *circ\_0001535* in AD patients. Then the GSEA method was used to screen out the pathways with significant enrichment differences between the high and low-expression groups. As shown in the Fig. 4, *circ\_0001535* was associated with six major pathways.

In addition, we further screened the genes with a high correlation with the expression of *circ\_0001535*. A total of 503 genes were screened which were significantly associated with *circ\_0001535* expression using Pearson correlation analysis at  $p < 0.05$  (Supplementary Table 4). This gene list was analyzed using Metascape Gene List Analysis for pathway and process enrichment using the following databases: KEGG Pathway, GO Biological Process, Reactome Gene Set, Canonical Pathways, CORUM, TRUST, DisGeNET, PaGenBase, Transcription. As shown in Fig. 5A, the top 20 clusters are shown here in descending order of  $-\text{Log}_{10}(p)$  values for their representative enriched terms (Fig. 5A). To further analyze the relationships between the clustered terms, a subset of each cluster was selected and visualized by Cytoscape to network its presentation as a network graph. Each node represents a rich term and is first colored by its cluster ID in these networks (Fig. 5B).

Furthermore, protein-protein interaction enrichment analysis was performed using the following databases: STRING, BioGrid, OmniPath and InWeb\_IM9. Only physical interactions in STRING (physical score  $> 0.132$ ) and

**Table 2. The results of correlation between *E2F1* and potential downstream genes and differential expression levels of downstream genes.**

Gene ID	Gene symbol	Correlation	$p$ -value	Log <sub>2</sub> FC	$p$ -value
1719	<i>DHFR</i>	-0.585	0.046	0.78351	0.038
2067	<i>ERCC1</i>	-0.603	0.038	-0.00035	0.997
2492	<i>FSHR</i>	0.658	0.020	0.558488	0.595
3090	<i>HIC1</i>	0.597	0.040	-0.16718	0.848
6241	<i>RRM2</i>	0.750	0.005	-1.62878	0.188
6502	<i>SKP2</i>	0.746	0.005	0.020207	0.942
7153	<i>TOP2A</i>	0.607	0.036	-0.78306	0.540

*E2F1*, E2F transcription factor 1; *DHFR*, dihydrofolate reductase; *ERCC1*, the excision repair cross-complementation group 1; *FSHR*, follicle-stimulating hormone receptor; *HIC1*, hypermethylated in cancer 1; *RRM2*, Ribonucleoside-Diphosphate Reductase Subunit M2; *SKP2*, S-phase kinase-associated protein 2; *TOP2A*, DNA topoisomerase II alpha.

BioGrid were used. The network contains a subset of proteins that form physical interactions with at least one other member of the list (Fig. 5C). The transcription factors in the network could also be considered potential and studied further.

### 3.5 Searching for Downstream Transcription Factors Regulated by *circ\_0001535*

In order to prove the potential transcription factors regulated by *circ\_0001535*, an analysis of transcription factors that may affect the expression of these genes using TRUST. The results revealed that *E2F1* is the key transcription factor. It may affect 7 genes: *DHFR*, *ERCC1*, *FSHR*, *HIC1*, *RRM2*, *SIP2* and *TOP2A* (Table 2, Fig. 6A). *DHFR* was the primary downstream gene that might be affected ( $p = 0.038$ ). Subsequently, the binding relationship between *E2F1* and *DHFR* was examined using JASPAR, and 2 binding sites were found to exist on chromosome 5 (Table 3, Fig. 6B).

### 3.6 The *circ\_0001535/E2F1/DHFR* Interaction was Identified in Vitro

SH-SY5Y cells were used as model cells to test the interaction relationship between *circ\_0001535* and its downstream regulators. A $\beta$  protein were added into SH-SY5Y cells to construct the AD cell model. Firstly, *circ\_0001535*, *E2F1* and *DHFR* expressions were evaluated using the RT-qPCR method. Results showed that the expressions of *circ\_0001535*, *E2F1* and *DHFR* were significantly higher in the AD cell model (Fig. 7A,  $p < 0.05$ ). Next, RIP and ChIP assays were processed to identify the binding relationship among circRNA, transcription factor and downstream effector gene in SH-SY5Y cells. RIP result showed *circ\_0001535* has a binding ship to *E2F1* (Fig. 7B,  $p < 0.05$ ). ChIP result showed *E2F1* could bind to *DHFR* promoter (Fig. 7C,  $p < 0.05$ ).

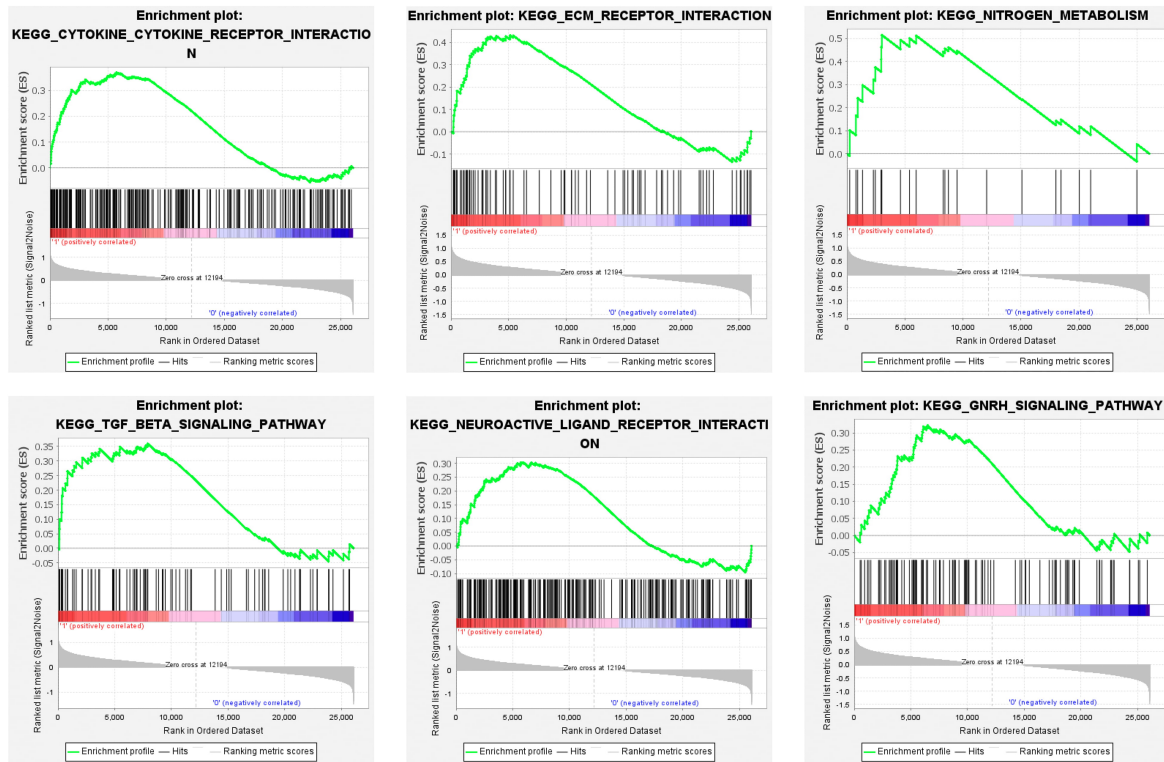


Fig. 4. GSEA applied to validate the hub gene signatures which were related to *circ\_0001535*. GSEA, gene set enrichment analysis.

Table 3. Binding sites between E2F1 and *DHFR* promoter.

Site	Score	TSS site	Start	End	Binding sequence
Site1	6.319671	NC_000005.10: c80626226-80624226	1571	1581	CGGGAGGCAGA
Site2	6.244307	NC_000005.10: c80626226-80624226	1163	1173	TGGGCGACAGA

TSS, transcription start site.

### 3.7 *Circ\_0001535* could Regulate Proliferation and Apoptosis through E2F1/DHFR Axis

Overexpression plasmids of *circ\_0001535* and si-RNA of *E2F1* and *DHFR* were created to identify biological functions of the *circ\_0001535/E2F1/DHFR* axis. First, the results of RT-qPCR showed that *circ\_0001535* overexpression could promote *DHFR* expression, while *E2F1* knock down could inhibit *DHFR* expression (Fig. 8A,  $p < 0.05$ ). Then, CCK-8 results showed *circ\_0001535*, *E2F1* and *DHFR* could down-regulate cell viability of AD cell model (Fig. 8B,  $p < 0.05$ ). In apoptosis assay, similar results could be observed, *circ\_0001535*, *E2F1* and *DHFR* all could promote cell apoptosis of the AD cell model (Fig. 8C,  $p < 0.05$ ).

## 4. Discussion

Numerous studies have suggested that non-coding RNA plays an important role in the diagnosis and pathogenesis of AD. Among them, circRNAs, as conserved non-coding RNA molecules, have great regulatory potential in various of neurodegenerative diseases [27–29]. In previous reports, circRNA profiles were constructed and used

to distinguish subjects with AD and mild cognitive impairment [30]. In the present study, circRNAs have been identified in RNA-seq data from the lateral temporal lobe of AD patients and elderly control. Differential expression analysis was performed in our study, and 12 dysregulated circRNAs were found between AD patients and elderly control. Among these circRNAs, 6 circRNAs were up-regulated, and 6 circRNAs were down-regulated in the group of AD patients. These circRNAs were chosen as candidate circRNAs for further research.

In order to evaluate diagnostic value of the 12 circRNAs, ROC curve analysis was processed. The results showed that 12 circRNAs have diagnostic potency. *Circ\_0006916* has been shown to play a female-specific role in the pathogenesis of AD [31]. Our results further indicated that *circ\_0006916* had a high diagnostic value in AD. In past studies, other circRNAs have been used to diagnose of non-neurodegenerative diseases. *Circ\_0000497* has been served as a potential biomarker for ovarian cancer [32]. For Hepatocellular carcinoma, some researchers found that *circ\_0001535* was up-regulated in cancer tissue [25]. *Circ\_0001380* was downregulated in the peripheral

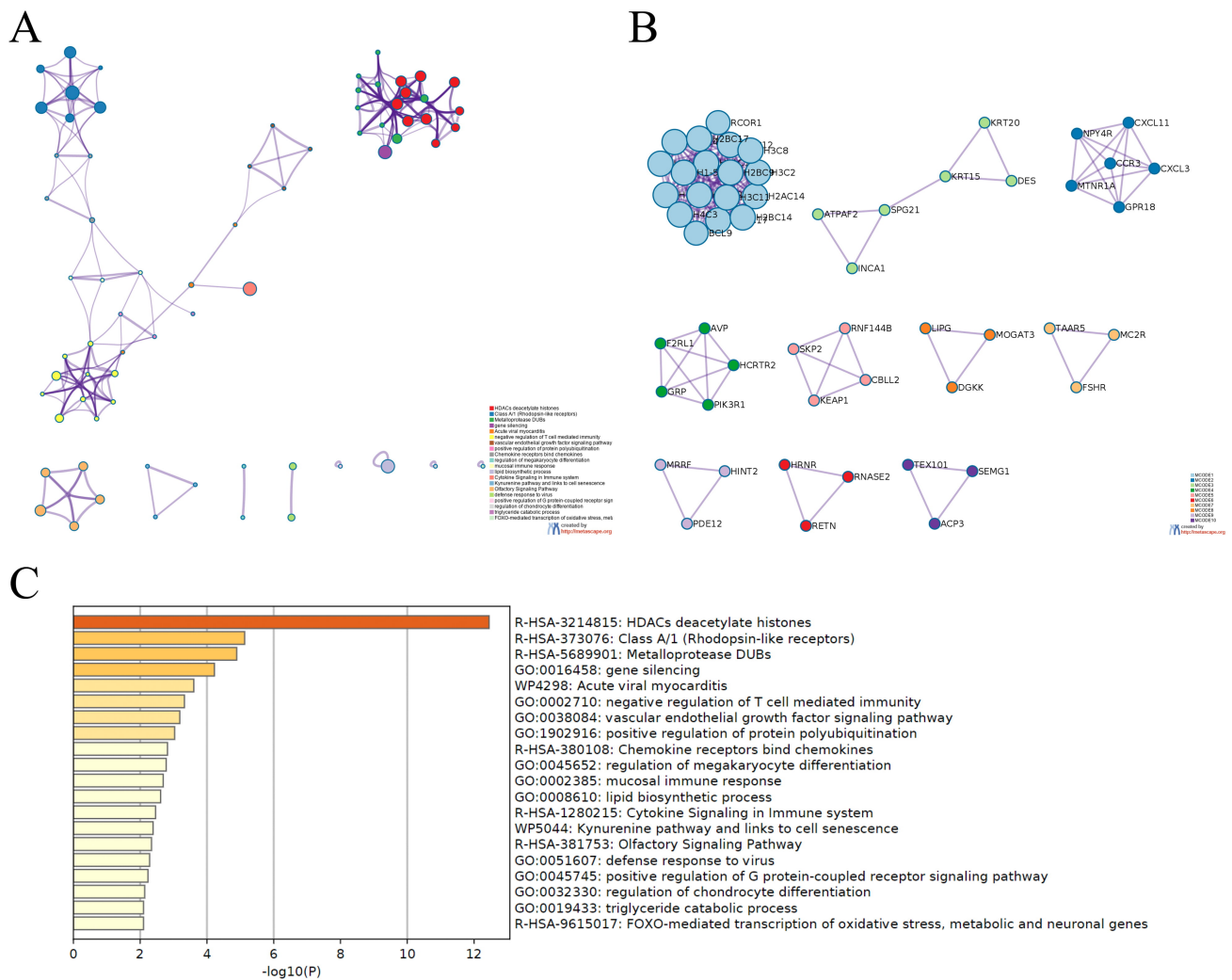


**Fig. 5. Metascape gene list analysis results shows pathways related to *circ\_0001535*.** (A) Network of enriched terms colored by cluster ID, where nodes that share the same cluster ID are typically close to each other. (B) Protein-protein interaction network and MCODE components identified in the gene lists. (C) Bar graph of enriched terms across input gene lists, colored by  $p$ -values. MCODE, molecular complex detection.

blood of patients with active pulmonary tuberculosis, and could serve as a diagnostic biomarker [33]. This study found these circRNAs were found to have significant diagnostic value for AD for the first time. These findings strongly supported that circRNAs were biomarkers for the diagnosis of AD.

In order to further clarify the expression difference of these circRNAs in AD patients and healthy participants, the expression levels of these circRNAs in cerebrospinal fluid were detected. The expression levels of 7 circRNAs were significantly differed between the control group and AD patients. Among these circRNAs, *circ\_0001535* had the highest AUC value and was significantly overexpressed in AD patients. In previous studies, ROC curve analysis of circRNAs predicting the risk of AD showed that the AUC value of most circRNAs was less than 0.85. Only a few circRNAs had AUC values greater than 0.85 [30,34]. These reports

further suggest that *circ\_0001535* has a high predictive value for the risk of AD. Hence, *circ\_0001535* was regarded as a key circRNA in the present study. The GSEA analysis was performed to further annotate the pathway related to the aberrantly expressed *circ\_0001535*. *Circ\_0001535* was associated with six major pathways which were closely related to AD disease progression [35–37]. The transforming growth factor beta (TGF- $\beta$ ) signaling pathway in the central nervous system has been identified in association with the host genes of circRNAs [38]. TGF- $\beta$  has been proven that it could ameliorate adult hippocampal neurogenesis in the AD model [39]. In this study, *circ\_0001535* was significantly enriched in the TGF- $\beta$  pathway. GnRH signaling was also linked to the malignant progression of AD [37]. Previous studies have not reported the correlation between GnRH signal and circRNA in AD. The present study first found the correlation between *circ\_0001535* and

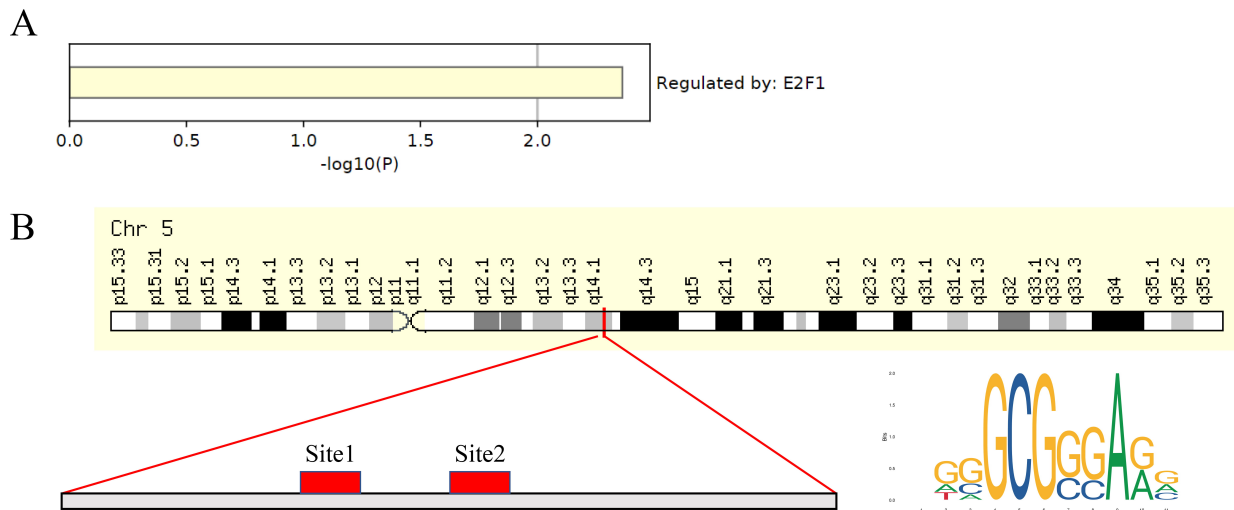


**Fig. 6.** TRRUST and JASPAR were used to find downstream genes effected by *circ\_0001535*. (A) Summary of enrichment analysis in TRRUST. (B) JASPAR analyze results shows two binding sites of *E2F1* on *DHFR*.

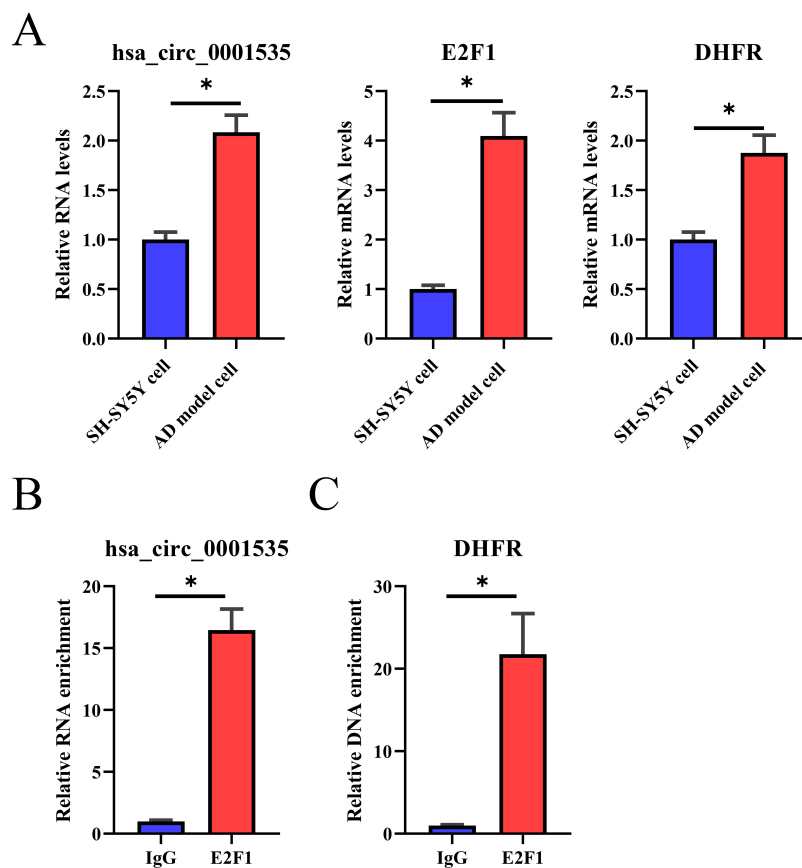


**Fig. 7.** Identification of regulation ship between *circ\_0001535* and its downstream regulators. (A) The differential expression of *circ\_0001535*, *E2F1* and *DHFR* between SH-SY5Y cells and AD model cells group was estimated by RT-qPCR. (B) RIP assay showed the regulation ship between *circ\_0001535* and *E2F1*. (C) ChIP assay showed the bind ship between *E2F1* and *DHFR*. \* $p < 0.05$  compared with SH-SY5Y cell group or IgG group. *DHFR*, dihydrofolate reductase.

GnRH signaling pathway. The above results indicate that *circ\_0001535* may play a key role in AD and the molecular mechanism of *circ\_0001535* regulating AD need to be further studied.

CircRNAs have been regarded as upstream effectors of some transcription factors and RNA-binding proteins to regulate cell proliferation and apoptosis [40]. However, in previous studies, no researchers have clarified the specific

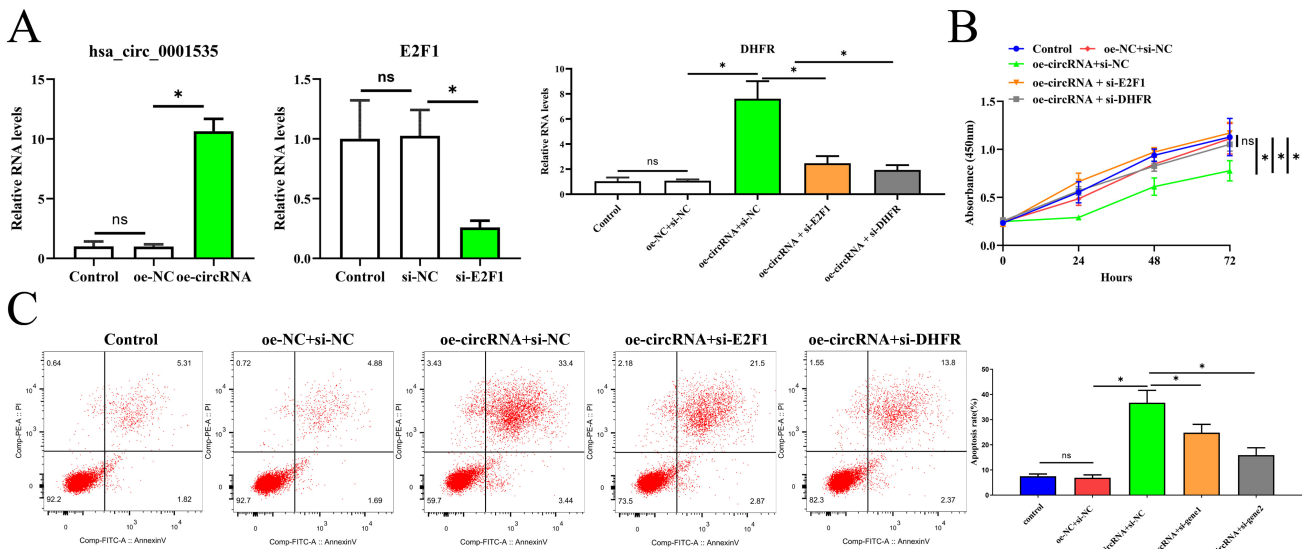


**Fig. 8. Identification of biological functions of *circ\_0001535/E2F1/DHFR* axis.** (A) The differential expression of *circ\_0001535*, *E2F1* and *DHFR* among different groups was estimated by RT-qPCR. (B) The proliferation ability of AD model cells in different groups was estimated by CCK-8 assay. (C) Flow cytometry were used to identify regulation ship of *circ\_0001535/E2F1/DHFR* axis on AD cell apoptosis. \* $p < 0.05$ . CCK8, Cell Counting Kit-8; NC, Negative control.

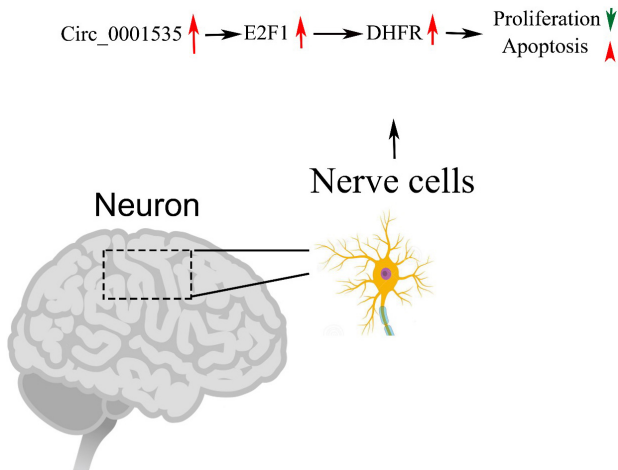


**Fig. 9. Schematic illustration of rationale to show the effect of *circ\_0001535* on AD cells by regulating *E2F1/DHFR* axis.**

regulating role of circRNAs on transcription factors in AD. In this study, we first found that *E2F1* was a candidate transcription factor that could be regulated by *circ\_0001535* (Fig. 9). In past studies, *E2F1* has been reported to regulate cognitive dysfunction of AD rats by regulating *NF-kB/GSK-3 $\beta$*  signaling axis [41]. Calpain-cleaved *E2F1* may also contribute to calpain-mediated neuronal damage [42]. These reports suggest that *E2F1* can regulate the cognitive dysfunction of AD. *Circ\_0001535* was positively correlated with *E2F1* in  $A\beta$ -treated SH-SY5Y cells. In addition, we demonstrated that *circ\_0001535* could inhibit the proliferation of AD cells by regulating *E2F1*. After that, in order to investigate the molecular mechanism of

*E2F1* regulating the biological activity of AD cells, we further searched for the downstream genes regulated by *E2F1* (Fig. 9). *DHFR* has been regarded as a key gene whose promoter region could be combined with *E2F1* in the present study. *DHFR* is a critical enzyme in folate metabolism and an important target of antineoplastic, antimicrobial, and anti-inflammatory drugs [43,44]. *DHFR* has been associated with developing certain neurodegenerative diseases in past reports. A transcriptome-wide association study in the Huntington's disease cohort found that increased *MSH3* and *DHFR* expression are associated with disease progression [45]. Some researchers also found that 20S proteasome isolated from the bovine brain directly hydrolyzes, *in vitro*, *DHFR*, demonstrated to be involved in the pathogenesis of neurodegenerative diseases [46]. In this study, *DHFR* was proven to inhibit the proliferation of SH-SY5Y cells. Hence, *circ\_0001535* as a key circRNA in this study has been found that it could inhibit proliferation and promote apoptosis of AD cells by regulating the *E2F1/DHFR* axis.

Further work is also needed to investigate possible functions of the circRNAs differentially abundant in AD vs. normal sample. First, the sample size was limited, which could have resulted in under- or over-estimation of the numbers of altered circRNAs. Therefore, larger sample sizes are needed to confirm our findings. Second, the molecular mechanism by which *circ\_0001535* regulates AD development has not been well understood. We did not find the downstream noncoding RNAs regulated by *circ\_0001535* in the present study. Our future studies, we will explore that the potential molecular mechanism of the *circ\_0001535/E2F1/DHFR* axis *in vivo*.

## 5. Conclusions

In summary, the expression levels of 7 circRNAs are correlated with the clinical features of patients with AD. Our findings provide important potential biomarkers for AD. Furthermore, *circ\_0001535* promotes A $\beta$ -induced apoptosis via *E2F1/DHFR* axis, suggesting a new insight into the pathogenesis of AD. These findings have the potential to provide important information about the role of specific circRNAs in the AD environment and point to specific future areas of therapeutic intervention in AD.

## Abbreviations

AD, Alzheimer's disease; CCK8, Cell Counting Kit-8; CHIP, Chromatin immunoprecipitation; circRNAs, circular RNAs; DHFR, dihydrofolate reductase; DMEM, Dulbecco's modified Eagle's medium; E2F1, E2F transcription factor 1; FBS, fetal calf serum; GEO, Gene Expression Omnibus; GSEA, Gene set enrichment analysis; lncRNA, long non-coding RNA; miR, microRNA; BED, Browser Extensible Data; TSS, transcription start site; NFTs, neurofibrillary tangles; oe, Overexpression; P/S, Penicillin/streptomycin; RIP, RNA Binding Protein Immunoprecipitation; ROC, Receiver operating characteristic curve; RT-qPCR, reverse transcription-quantitative PCR; si, Small interfering; TGF- $\beta$ , transforming growth factor beta.

## Availability of Data and Materials

The datasets used and/or analyzed during the current study are available from the corresponding author on reasonable request.

## Author Contributions

MM and JZ conceived and designed the study, revised the draft. JZ acquired fundings. MM and DX conducted the experiments. JZ wrote the first draft and revised the draft. MM and DX led statistical analysis and revised the draft. JZ led the revision of the draft. All authors contributed to editorial changes in the manuscript. All authors reviewed and approved the submitted version of the manuscript. All authors had complete access to all research data and assume complete responsibility for the data integrity and accuracy of the data analysis.

## Ethics Approval and Consent to Participate

The experiments were approved by the Medical Ethics Committee of Red Cross Hospital. The ethical statement No. is 202280. All subjects gave written informed consent in accordance with the Declaration of Helsinki.

## Acknowledgment

Not applicable.

## Funding

This study is supported by Zhejiang Traditional Chinese Medicine Science and Technology Project (2023004198).

## Conflict of Interest

The authors declare no conflict of interest.

## Supplementary Material

Supplementary material associated with this article can be found, in the online version, at <https://doi.org/10.31083/j.jin2204105>.

## References

- [1] Tejada Moreno JA, Villegas Lanau A, Madrigal Zapata L, Baena Pineda AY, Velez Hernandez J, Campo Nieto O, *et al.* Mutations in SORL1 and MTHFDL1 possibly contribute to the development of Alzheimer's disease in a multigenerational Colombian Family. *PLoS ONE*. 2022; 17: e0269955.
- [2] Li F, Qin W, Zhu M, Jia J. Model-Based Projection of Dementia Prevalence in China and Worldwide: 2020-2050. *Journal of Alzheimer's Disease*. 2021; 82: 1823–1831.
- [3] Vega IE, Cabrera LY, Wygant CM, Velez-Ortiz D, Counts SE. Alzheimer's Disease in the Latino Community: Intersection of Genetics and Social Determinants of Health. *Journal of Alzheimer's Disease*. 2017; 58: 979–992.
- [4] Ashraf A, So P. Spotlight on Ferroptosis: Iron-Dependent Cell Death in Alzheimer's Disease. *Frontiers in Aging Neuroscience*. 2020; 12: 196.
- [5] Kwak K, Stanford W, Dayan E, Alzheimer's Disease Neuroimaging Initiative. Identifying the regional substrates predictive of Alzheimer's disease progression through a convolutional neural network model and occlusion. *Human Brain Mapping*. 2022; 43: 5509–5519.
- [6] Wei J, Ma X, Nehme A, Cui Y, Zhang L, Qiu S. Reduced HGF/MET Signaling May Contribute to the Synaptic Pathology in an Alzheimer's Disease Mouse Model. *Frontiers in Aging Neuroscience*. 2022; 14: 954266.
- [7] Villa C, Stocco A. Epigenetic Peripheral Biomarkers for Early Diagnosis of Alzheimer's Disease. *Genes*. 2022; 13: 1308.
- [8] Ma L, He L, Kang S, Gu B, Gao S, Zuo Z. Advances in detecting N6-methyladenosine modification in circRNAs. *Methods*. 2022; 205: 234–246.
- [9] Wang L, Shui X, Mei Y, Xia Y, Lan G, Hu L, *et al.* miR-143-3p Inhibits Aberrant Tau Phosphorylation and Amyloidogenic Processing of APP by Directly Targeting DAPK1 in Alzheimer's Disease. *International Journal of Molecular Sciences*. 2022; 23: 7992.
- [10] Chanda K, Jana NR, Mukhopadhyay D. Long non-coding RNA MALAT1 protects against A $\beta$ <sub>1–42</sub> induced toxicity by regulating the expression of receptor tyrosine kinase EPHA2 via quenching miR-200a/26a/26b in Alzheimer's disease. *Life Sciences*. 2022; 302: 120652.
- [11] Liccardo F, Iaiza A, Śniegocka M, Masciarelli S, Fazi F. Circular RNAs Activity in the Leukemic Bone Marrow Microenvironment. *Non-Coding RNA*. 2022; 8: 50.
- [12] Xiao Y, Chen H, Liao J, Zhang Q, He H, Lei J, *et al.* The Potential Circular RNAs Biomarker Panel and Regulatory Networks of Parkinson's Disease. *Frontiers in Neuroscience*. 2022; 16: 893713.

- [13] Zheng D, Tahir RA, Yan Y, Zhao J, Quan Z, Kang G, *et al.* Screening of Human Circular RNAs as Biomarkers for Early Onset Detection of Alzheimer's Disease. *Frontiers in Neuroscience*. 2022; 16: 878287.
- [14] Zhang M, Bian Z. The Emerging Role of Circular RNAs in Alzheimer's Disease and Parkinson's Disease. *Frontiers in Aging Neuroscience*. 2021; 13: 691512.
- [15] Cochran KR, Veeraraghavan K, Kundu G, Mazan-Mamczarz K, Coletta C, Thambisetty M, *et al.* Systematic Identification of circRNAs in Alzheimer's Disease. *Genes*. 2021; 12: 1258.
- [16] Cao X, Guo J, Mochizuki H, Xu D, Zhang T, Han H, *et al.* Circular RNA circ\_0070441 regulates MPP<sup>+</sup>-triggered neurotoxic effect in SH-SY5Y cells via miR-626/IRS2 axis. *Metabolic Brain Disease*. 2022; 37: 513–524.
- [17] Chen W, Hou C, Wang Y, Hong L, Wang F, Zhang J. Circular RNA circTLK1 regulates dopaminergic neuron injury during Parkinson's disease by targeting miR-26a-5p/DAPK1. *Neuroscience Letters*. 2022; 782: 136638.
- [18] Wei R, Hu Q, Lu Y, Wang X. ceRNA Network Analysis Reveals AP-1 Transcription Factor Components as Potential Biomarkers for Alzheimer's Disease. *Current Alzheimer Research*. 2022; 19: 387–406.
- [19] Ren Z, Chu C, Pang Y, Cai H, Jia L. A circular RNA blood panel that differentiates Alzheimer's disease from other dementia types. *Biomarker Research*. 2022; 10: 63.
- [20] Lo I, Hill J, Vilhjálmsson BJ, Kjems J. Linking the association between circRNAs and Alzheimer's disease progression by multi-tissue circular RNA characterization. *RNA Biology*. 2020; 17: 1789–1797.
- [21] Zeng C, Xing H, Chen M, Chen L, Li P, Wu X, *et al.* Circ\_0049472 regulates the damage of A $\beta$ -induced SK-N-SH and CHP-212 cells by mediating the miR-107/KIF1B axis. *Experimental Brain Research*. 2022; 240: 2299–2309.
- [22] Meng T, Chen Y, Wang P, Yang L, Li C. Circ-HUWE1 Knockdown Alleviates Amyloid- $\beta$ -Induced Neuronal Injury in SK-N-SH Cells via miR-433-3p Release-Mediated FGF7 Downregulation. *Neurotoxicity Research*. 2022; 40: 913–924.
- [23] Mao Z, Lin D, Xu J. Hsa\_circ\_0001535 Regulates Colorectal Cancer Progression via the miR-433-3p/RBPJ Axis. *Biochemical Genetics*. 2022. (online ahead of print)
- [24] Bai L, Gao Z, Jiang A, Ren S, Wang B. Circ\_0001535 Facilitates Tumor Malignant Progression by miR-485-5p/LASP1 Axis in Colorectal Cancer. *Balkan Medical Journal*. 2022; 39: 411–421.
- [25] Zhang T, Jing B, Bai Y, Zhang Y, Yu H. Circular RNA circT-MEM45A Acts as the Sponge of MicroRNA-665 to Promote Hepatocellular Carcinoma Progression. *Molecular Therapy. Nucleic Acids*. 2020; 22: 285–297.
- [26] Writing Group of the Dementia and Cognitive Society of Neurology Committee of Chinese Medical Association; Alzheimer's Disease Chinese. Guidelines for dementia and cognitive impairment in China: the diagnosis and treatment of mild cognitive impairment. *Zhonghua Yi Xue Za Zhi*. 2010; 90: 2887–2893. (In Chinese)
- [27] Bigarré IM, Trombetta BA, Guo Y, Arnold SE, Carlyle BC. IGF2R circular RNA hsa\_circ\_0131235 expression in the middle temporal cortex is associated with AD pathology. *Brain and Behavior*. 2021; 11: e02048.
- [28] Chen D, Hao S, Xu J. Revisiting the Relationship Between Alzheimer's Disease and Cancer With a circRNA Perspective. *Frontiers in Cell and Developmental Biology*. 2021; 9: 647197.
- [29] Lu S, Yang X, Wang C, Chen S, Lu S, Yan W, *et al.* Current status and potential role of circular RNAs in neurological disorders. *Journal of Neurochemistry*. 2019; 150: 237–248.
- [30] Piscopo P, Manzini V, Rivabene R, Crestini A, Le Pera L, Pizzi E, *et al.* A Plasma Circular RNA Profile Differentiates Subjects with Alzheimer's Disease and Mild Cognitive Impairment from Healthy Controls. *International Journal of Molecular Sciences*. 2022; 23: 13232.
- [31] Urdánóz-Casado A, Sánchez-Ruiz de Gordo J, Robles M, Acha B, Roldan M, Zelaya MV, *et al.* Gender-Dependent Dereglulation of Linear and Circular RNA Variants of HOMER1 in the Entorhinal Cortex of Alzheimer's Disease. *International Journal of Molecular Sciences*. 2021; 22: 9205.
- [32] Luo N, Sulaiman Z, Wang C, Ding J, Chen Y, Liu B, *et al.* Hsa\_circ\_0000497 and hsa\_circ\_0000918 contributed to peritoneal metastasis of ovarian cancer via ascites. *Journal of Translational Medicine*. 2022; 20: 201.
- [33] Luo H, Peng Y, Luo H, Zhang J, Liu G, Xu H, *et al.* Circular RNA hsa\_circ\_0001380 in peripheral blood as a potential diagnostic biomarker for active pulmonary tuberculosis. *Molecular Medicine Reports*. 2020; 21: 1890–1896.
- [34] Li Y, Fan H, Sun J, Ni M, Zhang L, Chen C, *et al.* Circular RNA expression profile of Alzheimer's disease and its clinical significance as biomarkers for the disease risk and progression. *The International Journal of Biochemistry & Cell Biology*. 2020; 123: 105747.
- [35] Berezin V, Walmod PS, Filippov M, Dityatev A. Targeting of ECM molecules and their metabolizing enzymes and receptors for the treatment of CNS diseases. *Progress in Brain Research*. 2014; 214: 353–388.
- [36] Caraci F, Spampinato S, Sortino MA, Bosco P, Battaglia G, Bruno V, *et al.* Dysfunction of TGF- $\beta$ 1 signaling in Alzheimer's disease: perspectives for neuroprotection. *Cell and Tissue Research*. 2012; 347: 291–301.
- [37] Cáceres A, Vargas JE, González JR. APOE and MS4A6A interact with GnRH signaling in Alzheimer's disease: Enrichment of epistatic effects. *Alzheimer's & Dementia: the Journal of the Alzheimer's Association*. 2017; 13: 493–497.
- [38] Najafi S, Aghaei Zarch SM, Majidpoor J, Pordel S, Aghamiri S, Fatih Rasul M, *et al.* Recent insights into the roles of circular RNAs in human brain development and neurologic diseases. *International Journal of Biological Macromolecules*. 2022. (online ahead of print)
- [39] Wu X, Shen Q, Zhang Z, Zhang D, Gu Y, Xing D. Photoactivation of TGF $\beta$ /SMAD signaling pathway ameliorates adult hippocampal neurogenesis in Alzheimer's disease model. *Stem Cell Research & Therapy*. 2021; 12: 345.
- [40] Zhang Y, Zhao Y, Liu Y, Wang M, Yu W, Zhang L. Exploring the regulatory roles of circular RNAs in Alzheimer's disease. *Translational Neurodegeneration*. 2020; 9: 35.
- [41] Tuerxun M, Muhda A, Yin L. The molecular mechanisms of signal pathway activating effect of E2F-1/NF- $\kappa$ B/GSK-3 $\beta$  on cognitive dysfunction of Alzheimer rats. *Bioengineered*. 2021; 12: 10000–10008.
- [42] Zyskind JW, Wang Y, Cho G, Ting JH, Kolson DL, Lynch DR, *et al.* E2F1 in neurons is cleaved by calpain in an NMDA receptor-dependent manner in a model of HIV-induced neurotoxicity. *Journal of Neurochemistry*. 2015; 132: 742–755.
- [43] Lele AC, Mishra DA, Kamil TK, Bhakta S, Degani MS. Repositioning of DHFR Inhibitors. *Current Topics in Medicinal Chemistry*. 2016; 16: 2125–2143.
- [44] Raimondi MV, Randazzo O, La Franca M, Barone G, Vignoni E, Rossi D, *et al.* DHFR Inhibitors: Reading the Past for Discovering Novel Anticancer Agents. *Molecules*. 2019; 24: 1140.
- [45] Flower M, Lomeikaite V, Ciosi M, Cumming S, Morales F, Lo K, *et al.* MSH3 modifies somatic instability and disease severity in Huntington's and myotonic dystrophy type 1. *Brain*. 2019; 142: awz115.
- [46] Amici M, Sagratini D, Pettinari A, Pucciarelli S, Angeletti M, Eleuteri AM. 20S proteasome mediated degradation of DHFR: implications in neurodegenerative disorders. *Archives of Biochemistry and Biophysics*. 2004; 422: 168–174.